

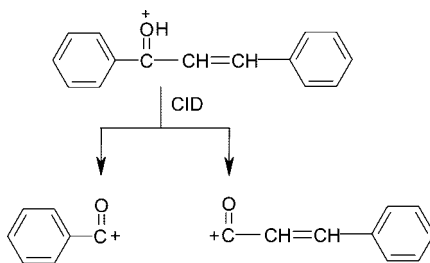
## Dissociative Protonation and Proton Transfers: Fragmentation of $\alpha, \beta$ -Unsaturated Aromatic Ketones in Mass Spectrometry

Nan Hu,<sup>†</sup> Ya-Ping Tu,<sup>\*,‡</sup> Yaqin Liu,<sup>†</sup> Kezhi Jiang,<sup>†</sup> and Yuanjiang Pan<sup>\*,†</sup>

Department of Chemistry, Zhejiang University, Hangzhou, Zhejiang 310027, China, and Drug Metabolism and Pharmacokinetics, Genelabs Technologies, 505 Penobscot Drive, Redwood City, California 94063

ytu@genelabs.com; panyuanjiang@zju.edu.cn

Received November 21, 2007



In mass spectrometry of the  $\alpha, \beta$ -unsaturated aromatic ketones,  $\text{Ph-CO-CH=CH-Ph}'$ , losses of a benzene from the two ends and elimination of a styrene are the three major fragmentation reactions of the protonated molecules. When the ketones are substituted on the right phenyl ring, the electron-donating groups are in favor of losing a styrene to form the benzoyl cation,  $\text{PhCO}^+$ , whereas the electron-withdrawing groups strongly favor loss of benzene of the left side to form a cinnamoyl cation,  $\text{Ph}'\text{CH=CHCO}^+$ . When the ketones are substituted on the left phenyl ring, the substituent effects on the reactions are reversed. In both cases, the ratios of the two competitive product ions are well-correlated with the  $\sigma_p^+$  substituent constants. Theoretical calculations indicate that the carbonyl oxygen is the most favorable site for protonation, and the olefinic carbon adjacent to the carbonyl is also favorable especially when a strong electron-releasing group is present on the right phenyl ring. The energy barrier to the interconversion between the ions formed from protonation at these two sites regulates the overall reactions. Transfer of a proton from the carbonyl oxygen to the *ipso* position on either phenyl ring, which is dissociative, triggers loss of benzene.

### Introduction

Protonation plays an important role in many chemical and enzymatic reactions. From the classic acid-catalyzed hydrolysis<sup>1</sup> of various small molecules to the enzyme–substrate interactions<sup>2</sup> in different biological systems, protonation of the small molecules or the enzymes is usually a critical step, and the

determination of the site of protonation is sometimes the key to understanding the reaction mechanism. A molecule, including very small ones such as carbon monoxide,<sup>3</sup> may be capable of accepting a proton at different positions. The thermodynamically favored site of protonation is primarily dependent upon the

<sup>†</sup> Zhejiang University.

<sup>‡</sup> Genelabs Technologies.

(1) (a) Cho, S. J.; Cui, C.; Lee, J. Y.; Park, J. K.; Suh, S. B.; Park, J.; Kim, B. H.; Kim, K. S. *J. Org. Chem.* **1997**, *62*, 4068–4071. (b) Jensen, M. P.; Halpern, J. *J. Am. Chem. Soc.* **1999**, *121*, 2181–2192. (c) Indurugalla, D.; Bennet, A. J. *J. Am. Chem. Soc.* **2001**, *123*, 10889–10898. (d) Fife, T. H.; Singh, R.; Bembli, R. *J. Org. Chem.* **2002**, *67*, 3179–3183. (e) Wu, Z.; Ban, F.; Boyd, R. J. *J. Am. Chem. Soc.* **2003**, *125*, 6994–7000. (f) Agnew, T. E.; Kim, H.-J.; Fishbein, J. C. *J. Phys. Org. Chem.* **2004**, *17*, 483–488. (g) Zahn, D. *Eur. J. Org. Chem.* **2004**, 4020–4023. (h) Mujika, J. I.; Mercero, J. M.; Lopez, X. *J. Am. Chem. Soc.* **2005**, *127*, 4445–4453. (i) Marlier, J. F.; Campbell, E.; Lai, C.; Weber, M.; Reinhardt, L. A.; Cleland, W. W. *J. Org. Chem.* **2006**, *71*, 3829–3836. (j) Brandao, T. A. S.; Orth, E. S.; Rocha, W. R.; Bortoluzzi, A. J.; Bunton, C. A.; Nome, F. *J. Org. Chem.* **2007**, *72*, 3800–3807.

(2) (a) Broo, K. S.; Brive, L.; Ahlberg, P.; Baltzer, L. *J. Am. Chem. Soc.* **1997**, *119*, 11362–11372. (b) Okimoto, N.; Tsukui, T.; Hata, M.; Hoshino, T.; Tsuda, M. *J. Am. Chem. Soc.* **1999**, *121*, 7349–7354. (c) Christensen, U. *Biochem. J.* **2000**, *349*, 623–628. (d) Vocadlo, D. J.; Wicki, J.; Rupitz, K.; Withers, S. G. *Biochemistry* **2002**, *41*, 9736–9746. (e) Klein, C. D.; Schiffmann, R.; Folkers, G.; Piana, S.; Rothlisberger, U. *J. Biol. Chem.* **2003**, *278*, 47862–47867. (f) Hunta, C.; Gillanib, N.; Faroneb, A.; Rezaeia, M.; Kline, P. C. *Biochim. Biophys. Acta* **2005**, *1751*, 140–149. (g) Tubert-Brohman, I.; Acevedo, O.; Jorgensen, W. L. *J. Am. Chem. Soc.* **2006**, *128*, 16904–16913. (h) Bizzarri, R.; Nifosi, R.; Abbruzzetti, S.; Rocchia, W.; Guidi, S.; Arosio, D.; Garau, G.; Campanini, B.; Grandi, E.; Ricci, F.; Viappiani, C.; Beltram, F. *Biochemistry* **2007**, *46*, 5494–5504.

(3) Rodriguez, C. F.; Cunje, A.; Hopkinson, A. C. *THEOCHEM* **1998**, *430*, 149–159.

(4) Hunter, E. P. L.; Lias, S. G. *J. Phys. Chem. Ref. Data* **1998**, *27*, 413–656.

proton affinity (PA)<sup>4</sup> at each local functionality of the molecule. However, it has been shown that the chemical environment, for example, the effect of the solvent<sup>5</sup> or the influence of a neighboring group,<sup>6</sup> also changes the pathway of protonation and the subsequent fragmentation.

Mass spectrometry has been a major tool among various experimental approaches for the measurement of the PA values<sup>4,7</sup> and for the determination of the site of protonation.<sup>8</sup> In the meantime, from the applicational perspective, information on how a molecule is protonated is valuable in structural determination, such as in the identification of drug metabolites,<sup>9</sup> using typically the electrospray ionization (ESI) mass spectrometry where the molecules of interest are protonated. Fragmentation reactions of the protonated molecules (MH<sup>+</sup>) are usually triggered by the positive charge formed upon protonation.<sup>10</sup> However, it is often found that when a molecule is protonated at the thermodynamically favored site, a “stable” molecular ion is formed leading to no fragmentations; in contrast, the MH<sup>+</sup> ion from which fragmentation takes place is often formed with the external proton added to an *unfavorable* position. The carboxylic acids, for example, are preferably protonated at the carbonyl oxygen, but water loss from the MH<sup>+</sup> ion occurs only when the proton migrates to the hydroxyl oxygen, which is the disadvantageous site for protonation.<sup>11</sup> Likewise, for the esters, loss of the alcohol proceeds from the MH<sup>+</sup> ion where the proton is located on the alkoxy oxygen even though protonation at the carbonyl oxygen is energetically preferred.<sup>12</sup> As the essential functional group of peptides, the amide linkage has been studied extensively for its protonation and the subsequent fragmentation. Both theoretical and experimental investigations<sup>13,14</sup> have unanimously testified that protonation of the amides at the carbonyl oxygen is favorable in energy, whereas the decomposing configuration of the MH<sup>+</sup> ion, which has the proton at the nitrogen, is produced after surmounting a high energy barrier that exists between the two isomeric forms.<sup>13</sup> From the stable initial structure to the unstable

dissociative structure, proton migration required for the fragmentation reaction has been witnessed in many cases as in carboxylic acids and their derivatives. This has led to the discovery of the mobile proton model<sup>15</sup> that is now routinely applied to the mass spectrometry of peptides and proteins.

Migration of the proton (and other small cations),<sup>16</sup> as a prelude of the mobile proton theory, was observed earlier in many rigid aromatic molecules by Grutzmacher and co-workers.<sup>17</sup> On the benzene, naphthalene, phenanthrene, biphenyl, or terphenyl rings, the ionizing proton, which is specifically attached to the oxygen of a carbonyl group on one end of the molecules, migrates *across the rings* to the other end where it hits a methoxymethyl group (at the oxygen) to eliminate a neutral methanol. From these same precursor ions, another reaction to the formation of the methoxymethyl cation indicates migration of the proton to the *ipso* position.<sup>17</sup> These footprints have exposed the mobile characteristic of the proton. However, what is important behind these observations and the mobile proton model is the fact that a dissociation reaction occurs *only* when the proton is attached to a specific position of the molecule.

We are interested in identifying the positions of a molecule where the arrival of a proton triggers fragmentation of the MH<sup>+</sup> ions and believe that this is an important initial step in the interpretation of the mass spectra. These positions are *not* necessarily the most basic site (i.e., their local proton affinity may be even *lower* than that at other positions). However, upon capture of a proton at these sites, fragmentation takes place immediately with *no more* further hydrogen shift. Therefore, they are truly the “hot spots” of the protonated molecules. Benzamides are preferably protonated at the carbonyl oxygen.<sup>18</sup> However, a major reaction to eliminate an isocyanate (O=C=NR) requires protonation on the phenyl ring at the C<sub>1</sub>-position to which the carbonyl group is attached.<sup>19</sup> Similarly, benzophenones, acetophenones, and dibenzyl ethers are all preferentially protonated at the oxygen, but the retro-Friedel-Crafts deacylation or dealkylation reaction, which is the dominant pathway, requires that the C<sub>1</sub>-position of the phenyl ring be protonated.<sup>20</sup> The C<sub>1</sub>-positions in these molecules are described previously by one of us<sup>20</sup> as the dissociative protonation sites.

To continue these efforts, we recently studied the reactions of  $\alpha,\beta$ -unsaturated aromatic ketones, the chalcones, in mass spectrometry, and the results are presented in this paper. With a vinyl unit between the carbonyl and the phenyl groups, which

(5) (a) Raczyńska, E. D.; Darowska, M.; Cyranski, M. K.; Makowski, M.; Rudka, T.; Gal, J.-F.; Maria, P.-C. *J. Phys. Org. Chem.* **2003**, *16*, 783–796. (b) Raczyńska, E. D.; Makowski, M.; Gornicka, E.; Darowska, M. *Int. J. Mol. Sci.* **2005**, *6*, 143–156. (c) Hilal, R.; Elroby, S. A. K. *Int. J. Quantum Chem.* **2005**, *103*, 449–459. (d) Alagona, G.; Ghio, C. *THEOCHEM* **2007**, *811*, 223–240.

(6) (a) Hu, W.; Reder, E.; Hesse, M. *Helv. Chim. Acta* **1996**, *79*, 2137–2151. (b) Tu, Y.-P.; Harrison, A. G. *J. Am. Soc. Mass Spectrom.* **1998**, *9*, 454–462. (c) Cox, C.; Lectka, T. *Org. Lett.* **1999**, *1*, 749–752. (d) Reid, G. E.; Simpson, R. J.; O’Hair, R. A. J. *J. Am. Soc. Mass Spectrom.* **2000**, *11*, 1047–1060. (e) Zhao, J.; Shoeib, T.; Siu, K. W. M.; Hopkinson, A. C. *Int. J. Mass Spectrom.* **2006**, *255/256*, 265–278.

(7) (a) Harrison, A. G. *Mass Spectrom. Rev.* **1997**, *16*, 201–217. (b) Cooks, R. G.; Wong, P. S. H. *Acc. Chem. Res.* **1998**, *31*, 379–386.

(8) (a) Raczyńska, E. D.; Rudka, T.; Darowska, M.; Dabkowska, I.; Gal, J.-F.; Maria, P.-C. *J. Phys. Org. Chem.* **2005**, *18*, 856–863. (b) Kone, M.; Illien, B.; Laurence, C.; Gal, J.-F.; Maria, P.-C. *J. Phys. Org. Chem.* **2006**, *19*, 104–114. (c) Kabli, S.; van Beelen, E. S. E.; Ingemann, S.; Henriksen, L.; Hammerum, S. *Int. J. Mass Spectrom.* **2006**, *249/250*, 370–378. (d) Bouchoux, G. *Mass Spectrom. Rev.* **2007**, *26*, 775–835.

(9) (a) Kostianen, R.; Kotiao, T.; Kuuranne, T.; Auriola, S. *J. Mass Spectrom.* **2003**, *38*, 357–372. (b) Feng, W. Y. *Curr. Drug Discovery Technol.* **2004**, *1*, 295–312. (c) Chen, Y.; Monshouwer, M.; Fitch, W. L. *Pharm. Res.* **2007**, *24*, 248–257. (d) Prakash, C.; Shaffer, C. L.; Nedderman, A. *Mass Spectrom. Rev.* **2007**, *26*, 340–369.

(10) Wysocki, V. H.; Tsapraillis, G.; Smith, L. L.; Breci, L. A. *J. Mass Spectrom.* **2000**, *35*, 1399–1406.

(11) (a) Benoit, F. M.; Harrison, A. G. *J. Am. Chem. Soc.* **1977**, *99*, 3980–3984. (b) Middlemiss, N. E.; Harrison, A. G. *Can. J. Chem.* **1979**, *57*, 2827–2833.

(12) (a) Denekamp, C.; Stanger, A. *J. Mass Spectrom.* **2002**, *37*, 336–342. (b) Opitz, J. *Int. J. Mass Spectrom.* **2007**, *265*, 1–14.

(13) Lin, H. Y.; Ridge, D. P.; Uggerud, E.; Vulpius, T. *J. Am. Chem. Soc.* **1994**, *116*, 2996–3004.

(14) (a) Zahm, D. *J. Phys. Chem. B* **2003**, *107*, 12303–12306. (b) Day, V. W.; Hossain, M. A.; Kang, S. O.; Powell, D.; Lushington, G.; Bowman-James, K. *J. Am. Chem. Soc.* **2007**, *129*, 8692–8693.

(15) (a) Johnson, R. S.; Krylov, D.; Walsh, K. A. *J. Mass Spectrom.* **1995**, *30*, 386–387. (b) Dongre, A. R.; Jones, J. L.; Somogyi, A.; Wysocki, V. H. *J. Am. Chem. Soc.* **1996**, *118*, 8365–8374. (c) Harrison, A. G.; Yalcin, T. *Int. J. Mass Spectrom. Ion Processes* **1997**, *165/166*, 339–347. (d) Csonka, I. P.; Paizs, B.; Lendvay, G.; Suhai, S. *Rapid Commun. Mass Spectrom.* **2000**, *14*, 417–431. (e) Paizs, B.; Suhai, S. *Mass Spectrom. Rev.* **2005**, *24*, 508–548. (f) Polfer, N. C.; Oomens, J.; Suhai, S.; Paizs, B. *J. Am. Chem. Soc.* **2007**, *129*, 5887–5897. (g) Lioe, H.; Laskin, J.; Reid, G. E.; O’Hair, R. A. J. *J. Phys. Chem. A* **2007**, *111*, 10580–10588.

(16) For a review on hydrogen scrambling, see: Kuck, D. *Int. J. Mass Spectrom. Ion Processes* **2002**, *213*, 101–144.

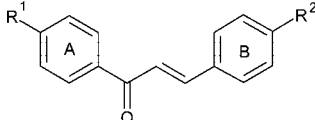
(17) (a) Filges, U.; Grutzmacher, H.-F. *Org. Mass Spectrom.* **1986**, *21*, 673–680. (b) Filges, U.; Grutzmacher, H.-F. *Org. Mass Spectrom.* **1987**, *22*, 444–450. (c) Filges, U.; Grutzmacher, H.-F. *Int. J. Mass Spectrom. Ion Processes* **1988**, *83*, 93–109. (d) Grutzmacher, H.-F.; Thielking, G. *Org. Mass Spectrom.* **1988**, *23*, 397–405. (e) Grutzmacher, H.-F.; Thielking, G.; Wittneben, D.; Eikenberg, D. *Int. J. Mass Spectrom. Ion Processes* **1990**, *98*, 259–268. (f) Thielking, G.; Filges, U.; Grutzmacher, H.-F. *J. Am. Soc. Mass Spectrom.* **1992**, *3*, 417–426.

(18) (a) Catalan, J.; Yanez, M. *Tetrahedron* **1980**, *36*, 665–667. (b) Grutzmacher, H.-F.; Caltapanides, A. *J. Am. Soc. Mass Spectrom.* **1994**, *5*, 826–836.

(19) Tu, Y.-P. *Rapid Commun. Mass Spectrom.* **2004**, *18*, 1345–1351.

(20) Tu, Y.-P. *J. Org. Chem.* **2006**, *71*, 5482–5488.

CHART 1



Series I			Series II		
R <sup>1</sup> = H	R <sup>2</sup>	M.W.	R <sup>2</sup> = H	R <sup>1</sup>	M.W.
1	H	208	10	NO <sub>2</sub>	253
2	F	226	11	CF <sub>3</sub>	276
3	Cl	242	12	Cl	242
4	Br	286	13	CH <sub>3</sub>	222
5	NO <sub>2</sub>	253	14	OCH <sub>3</sub>	238
6	CF <sub>3</sub>	276	15	NH <sub>2</sub>	223
7	CH <sub>3</sub>	222			
8	OCH <sub>3</sub>	238			
9	N(CH <sub>3</sub> ) <sub>2</sub>	251			

is an additional site with high PA, protonation at unfavorable sites that induces fragmentation was observed. In addition, the MH<sup>+</sup> ions of selected chalcones with the proton unambiguously attached to a specific position were prepared by in situ fragmentation of larger precursor molecules; in the reactions of these species and the deuterated counterparts, it was clearly observed that the proton was floating in the molecular ions.

## Results and Discussion

In the collision-induced dissociation (CID) mass spectra of the MH<sup>+</sup> ions of all the chalcone compounds studied (Chart 1), losses of benzene from the two ends and loss of styrene (containing the B-ring) were observed, along with other minor reactions. As an example, Figure 1 shows the spectrum for compound 7 that bears a methyl substituent on the B-ring. The major product ions, *m/z* 145, 131, and 105, are formed as a result of the elimination of benzene (A-ring), methylbenzene (B-ring), and *p*-methylstyrene, respectively. For chalcone 1 that is unsubstituted, the two losses of benzene (A- or B-ring) are indistinguishable and not discussed. Data for all compounds studied are summarized in Table S1 in the Supporting Information.

**Protonation-Induced Fragmentation.** The chalcone molecules may be protonated at multiple positions, including the carbonyl oxygen, either carbon of the vinyl unit, the phenyl rings, and the substituent when it has a heteroatom. The preferred site for protonation of these molecules has not been

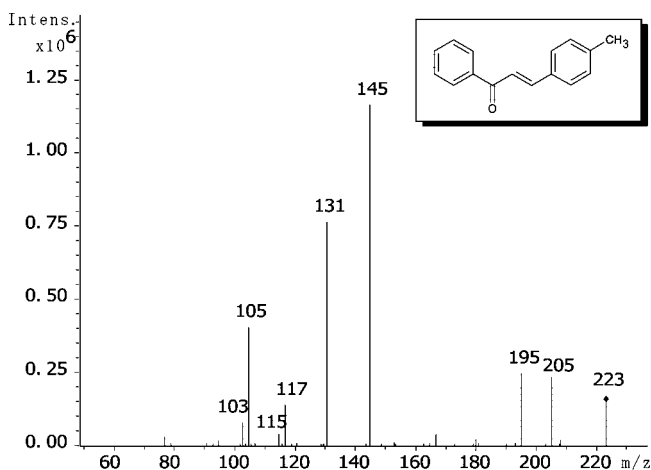
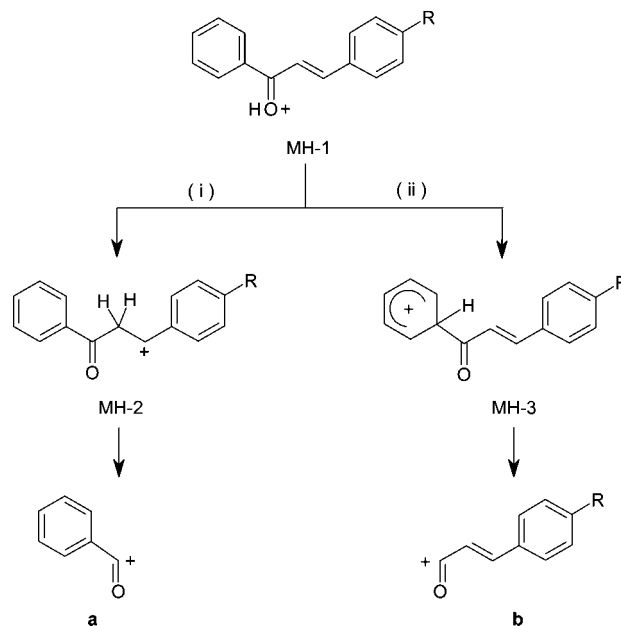


FIGURE 1. CID mass spectrum of the MH<sup>+</sup> ion (*m/z* 223) of chalcone 7.

TABLE 1. PA Values and Possible Site of Protonation of Selected Compounds

compound	PA (kcal/mol) <sup>4</sup>	site of protonation
C <sub>6</sub> H <sub>6</sub>	179.3	C <sup>21</sup>
C <sub>6</sub> H <sub>5</sub> -CHO	199.3	O <sup>22</sup>
C <sub>6</sub> H <sub>5</sub> -C(=O)CH <sub>3</sub>	205.8	O <sup>23</sup>
C <sub>6</sub> H <sub>5</sub> -CH=CH <sub>2</sub>	200.6	C(H <sub>2</sub> ) <sup>24</sup>
C <sub>6</sub> H <sub>5</sub> -C(CH <sub>3</sub> )=CH <sub>2</sub>	206.5	C(H <sub>2</sub> ) <sup>25</sup>
4-CF <sub>3</sub> -C <sub>6</sub> H <sub>4</sub> -C(CH <sub>3</sub> )=CH <sub>2</sub>	197.3	C(H <sub>2</sub> )
4-O <sub>2</sub> N-C <sub>6</sub> H <sub>4</sub> -C(CH <sub>3</sub> )=CH <sub>2</sub>	194.9	C(H <sub>2</sub> )
4-CH <sub>3</sub> O-C <sub>6</sub> H <sub>4</sub> -C(CH <sub>3</sub> )=CH <sub>2</sub>	217.7	C(H <sub>2</sub> )
4-(CH <sub>3</sub> ) <sub>2</sub> N-C <sub>6</sub> H <sub>4</sub> -C(CH <sub>3</sub> )=CH <sub>2</sub>	230.5	C(H <sub>2</sub> )

SCHEME 1



determined yet. However, based on the proton affinities of related molecules given in Table 1 (the first 4 entries), we believe that the carbonyl oxygen is the most favorable site for protonation giving rise to the MH-1 ion, as shown in Scheme 1. The vinyl carbon adjacent to the carbonyl group is rather competitive, whereas the C<sub>1</sub>-position of ring A to which the carbonyl is attached would be difficult to be protonated directly. Proton transfers from the oxygen to these two less favorable sites leading to MH-2 and MH-3, respectively, would have certain energy barriers but are necessary for the subsequent fragmentation reactions to proceed. Direct cleavage induced by the formal positive charge in MH-2 gives rise to a neutral styrene and the C<sub>6</sub>H<sub>5</sub>CO<sup>+</sup> ion **a** and elimination of benzene from MH-3 results in the cinnamoyl cation **b**.

In the chalcones, the PA at the C<sub>1</sub>-position (ring A) should be similar to that of benzene (or slightly lower due to the destabilizing effects of the carbonyl). In contrast, the PA at the carbonyl oxygen is expected to be close to that of acetophenone, that is, 20–25 kcal/mol higher than that at the C<sub>1</sub>-position (Table 1). Therefore, the 1,3-proton transfer from MH-1 to MH-3 is a considerably endothermic process. Interestingly, ion **b** formed

(21) Kuck, D. *Mass Spectrom. Rev.* **1990**, *9*, 583–630.

(22) Lau, Y. K.; Kebarle, P. *J. Am. Chem. Soc.* **1976**, *98*, 7452–7453.

(23) (a) Hegedus-Vajda, J.; Harrison, A. G. *Int. J. Mass Spectrom. Ion Phys.* **1979**, *30*, 293–306. (b) Bouchoux, G.; Djazi, F.; Houriet, R.; Rolli, E. *J. Org. Chem.* **1988**, *53*, 3498–3501. (c) Wolf, R.; Grutzmacher, H.-F. *New J. Chem.* **1990**, *4*, 379–382.

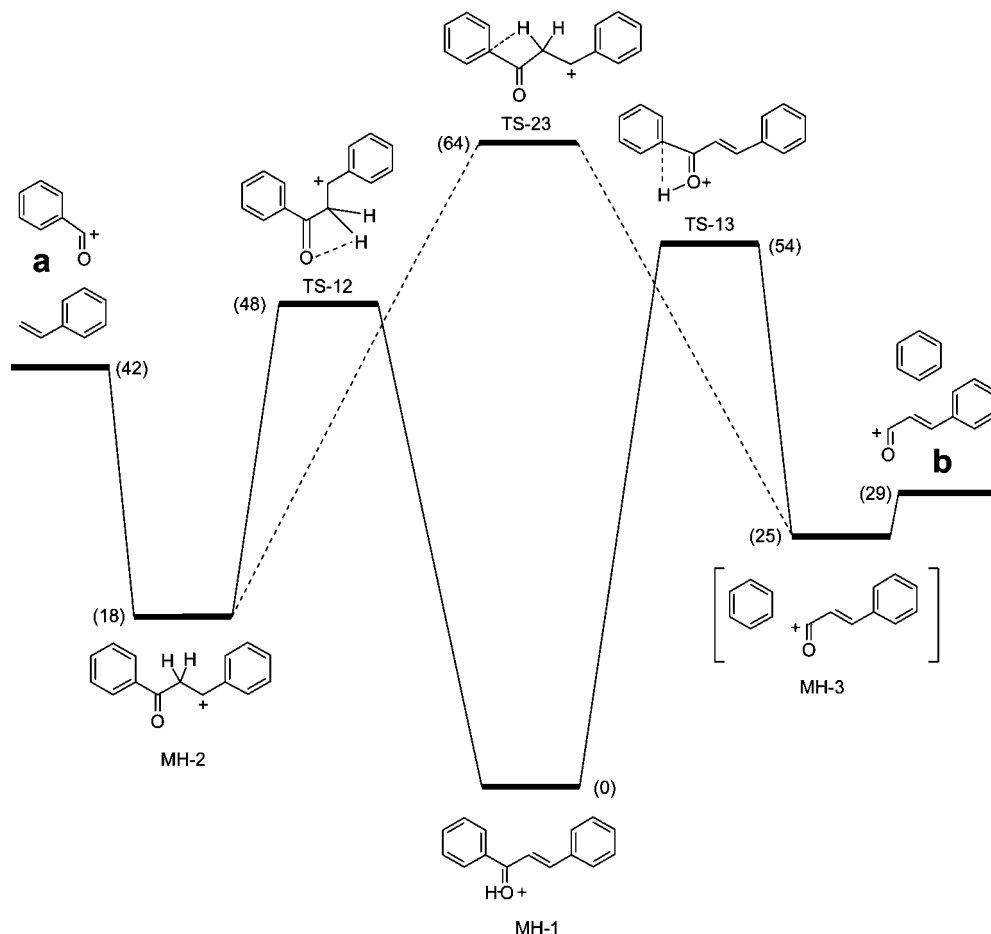


**FIGURE 2.** Potential energy diagram for the reactions of the  $MH^+$  ion of the unsubstituted chalcone calculated using DFT at the RB3LYP/6–31G(d) level of theory. Relative energies are given in kcal/mol in the parentheses.

via this proton transfer is still the *dominant* product, as seen at  $m/z$  145 in Figure 1 for compound **7**, despite the pronounced endothermicity and a possible high energy barrier to the 1,3-H shift.<sup>13</sup>

To quantitatively describe the energy requirements of the reactions, theoretical calculations were carried out using the density functional theory (DFT) at the RB3LYP/6–31G(d) level of theory, and a potential energy surface was obtained for the unsubstituted chalcone. As shown in Figure 2, MH-1 is the most stable species, and MH-2 and MH-3 are higher in energy by 18 and 25 kcal/mol, respectively, as expected. MH-3 exists as an ion-neutral complex in a shallow energy well (to be discussed afterward). Transition state TS-12 is 6 kcal/mol lower in energy than TS-13, and TS-23 is 10 kcal/mol above TS-13. The total energy of products for the reaction to form ion **a** is 13 kcal/mol higher than that for the reaction to give ion **b**.

When the  $MH^+$  ions are formed in atmospheric pressure chemical ionization, they are stabilized after many collisions with the background gas molecules<sup>26</sup> and reside in the deep energy well mostly as MH-1 in the ground state. Upon collisional activation, their internal energy<sup>27</sup> increases to overcome energy barriers to the fragmentations. In general, when

the transition states for two competing reactions are close in energy, the stability of the products could be the driving force for the reactions; when the transition states are much differentiated in energy, the transition states take control of the reactions regardless of the product thermochemistry.

The stability of all ionic species may vary to some extent as the substituent changes. When the chalcones are substituted on the B-ring, the substituent influence on MH-2 in particular should be remarkable since the conjugating system is interrupted by the newly formed  $CH_2$  group in the middle that turns MH-2 to a substituted benzyl cation. The difference in energy between MH-1 and MH-2 for the unsubstituted chalcone is 18 kcal/mol (Figure 2); however, the energy difference between these two species is much narrowed to be only 8 kcal/mol for chalcone **9** that bears an *N,N*-dimethylamino group on the B-ring (see Table S4 in the Supporting Information). This indicates that MH-2 is much *more sensitive* than MH-1 to structural changes on the B-ring. Likewise, TS-12 is also expected to be *more sensitive* than TS-13 to these changes. In fact, the substituent effect on the stability of MH-2 and TS-12 is in parallel to the effect on the proton affinity of the styrenes (protonated styrenes are benzyl cations as well). For the styrenes included in Table 1 with a substituent on the para position (note

(24) (a) Mathews, P. J.; Stone, J. A. *Can. J. Chem.* **1988**, *66*, 1239–1248. (b) Kafafi, S. A.; Meot-Ner (Mautner), M.; Liebman, J. F. *Struct. Chem.* **1990**, *1*, 101–105.

(25) (a) Harrison, A. G.; Houriet, R.; Tidwell, T. T. *J. Org. Chem.* **1984**, *49*, 1302–1304. (b) Pytel, O.; Trlida, B. *Collect. Czech. Chem. Commun.* **2007**, *72*, 1025–1036.

(26) (a) Schneider, B. B.; Chen, D. D. Y. *Anal. Chem.* **2000**, *72*, 791–799. (b) Schneider, B. B.; Douglas, D. J.; Chen, D. D. Y. *Rapid Commun. Mass Spectrom.* **2001**, *15*, 249–257. (c) Tu, Y.-P.; He, L.; Fitch, W.; Lam, M. *J. Org. Chem.* **2005**, *70*, 5111–5118.

(27) Gabelica, V.; De Pauw, E. *Mass Spectrom. Rev.* **2005**, *24*, 566–587.

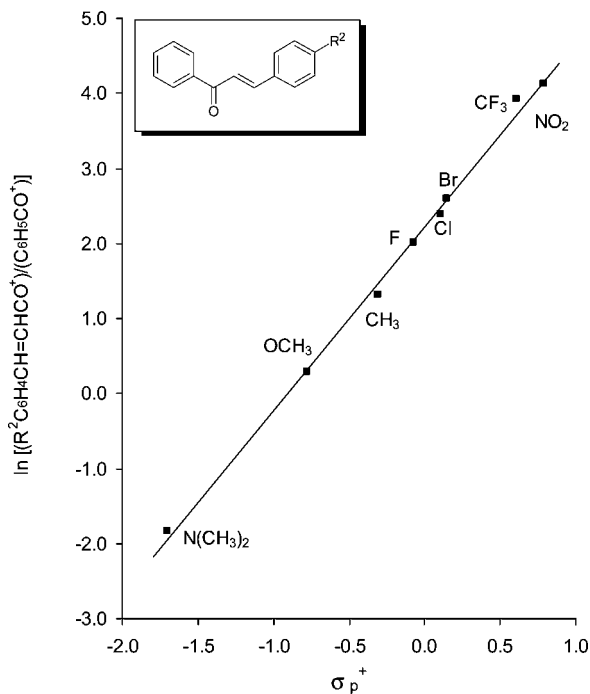


**FIGURE 3.** Relationship of  $\ln[(R^2C_6H_4CH=CHCO^+)/C_6H_5CO^+]$  with the  $\sigma_p^+$  substituent constants in the fragmentation of protonated chalcones substituted on the B-ring. Note that the substituted cinnamoyl ion is the numerator.

that all data for those without a  $CH_3$  on the vinyl are not available), it is clear that electron-donating groups ( $CH_3O$  and  $(CH_3)_2N$ ) significantly increase the proton affinity by stabilizing the  $MH^+$  ions of styrenes and electron-withdrawing groups ( $CF_3$  and  $NO_2$ ) strongly decrease the proton affinity by destabilizing the  $MH^+$  ions.

To further understand the roles of various  $MH^+$  ions and transition states in the fragmentation reactions, the mass spectrometry of two series of chalcones with different substituents on ring A or B (Chart 1) was then characterized. For series I with an R on the B-ring, it was found that all the electron-attracting groups favored formation of ion **b** to eliminate the A-ring benzene, whereas the electron-releasing groups were in favor of losing the B-ring styrene to form ion **a**, as indicated by the relationship of the intensity ratios<sup>28</sup> of these two competitive product ions (**b** over **a**) with the  $\sigma_p^+$  substituent constants<sup>29</sup> shown in Figure 3. The competition of the two reactions is in line with the sensitivity of the two transition states (TS-12 and TS-13) to structural changes. When an electron-releasing group is present on the B-ring, the energy barrier (TS-12) to the  $MH-1 \rightarrow MH-2$  process is lowered, and direct cleavage resulting in ion **a** is dominant. In contrast, when an electron-attracting group is attached, the same energy barrier is elevated, then the alternative pathway via TS-13 prevails to form ion **b**. This clearly demonstrates that the transition state TS-12 plays a unique role as a “regulator” in the overall reactions of series I chalcones.

As for the chalcones in series II, the substituents that are on the A-ring exhibited different effect than in series I on the

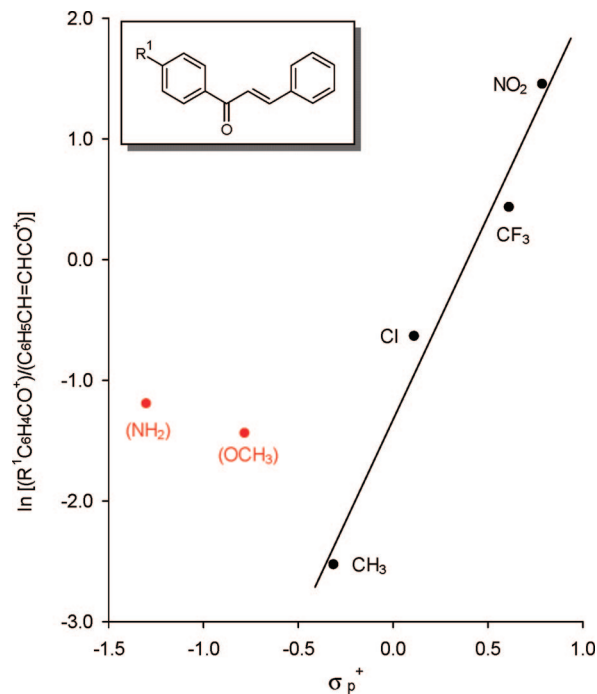
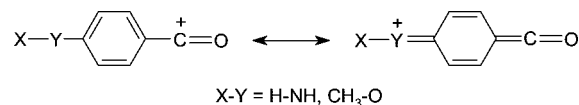


**FIGURE 4.** Relationship of  $\ln[(R^1C_6H_4CH=CHCO^+)/C_6H_5CH=CHCO^+]$  with the  $\sigma_p^+$  substituent constants in the fragmentation of protonated chalcones substituted on the A-ring. Note that the cinnamoyl ion is the denominator.

#### SCHEME 2



reactions. The  $MH-1$  ion<sup>30</sup> and TS-13 are now more sensitive to structural changes on the A-ring, whereas  $MH-2$  and TS-12 are less sensitive to these changes. This is because the charge site in the former pair is attached to the A-ring where the substituent changes, but the charge in the latter pair is shielded by the  $CH_2$  unit in the middle. Therefore, for this series of chalcones, transition state TS-13 takes over the “regulator” role. Qualitatively, electron-releasing groups stabilize TS-13 and cut the energy barrier to the  $MH-1 \rightarrow MH-3$  process, thus favoring formation of the cinnamoyl ion **b**. On the other hand, electron-withdrawing groups destabilize TS-13 and further raise the energy barrier to same reaction, allowing the other pathway toward ion **a** to prevail. As shown in Figure 4, the intensity ratios<sup>28</sup> of the two competitive product ions (**a** over **b** in this series) correlate well with the substituent constants in general. However, the two outliers indicate that other factors also played an important role in the reactions. We initially expected that both  $NH_2$  and  $OCH_3$  should considerably stabilize TS-13, as observed previously in benzophenones,<sup>20</sup> and thus strongly favor loss of the A-ring benzenes. In fact, the benzoyl cations **a** ( $R = NH_2$  or  $OCH_3$ ) can also be stabilized by the quinone resonance forms, as depicted in Scheme 2. This additional stabilization elevated the intensity of the **a** ions and thus brought the two compounds off the general linear correlation with the substituent constants.

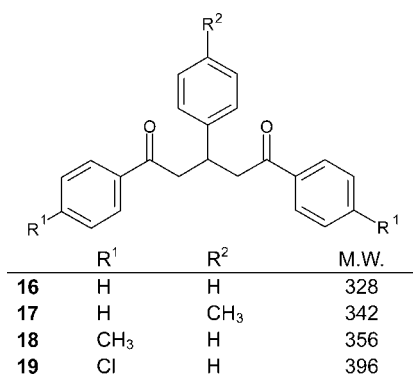
**Proton Transfers.** From the fragmentation of two series of chalcones, we found that  $MH-1$  is the most stable species, and

(28) The intensity ratios are for ions **b** over **a** in Figure 3, and reversed to **a** over **b** in Figure 4 to keep the slope positive. Intensities are corrected for secondary fragmentations.

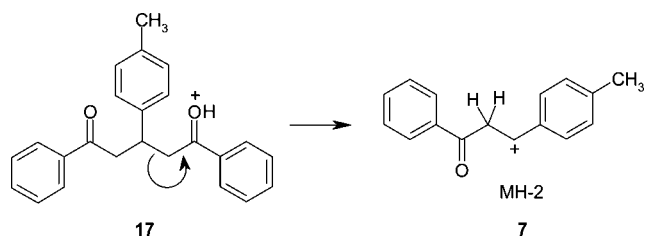
(29) Hansch, C.; Leo, A.; Taft, R. W. *Chem. Rev.* **1991**, *91*, 165–195.

(30) For series II, the structures of  $MH-1$ ,  $MH-2$ , and  $MH-3$  are the same as shown in Scheme 1 except that the substituent R is on the left A-ring.

CHART 2



SCHEME 3



intramolecular proton transfer leading to the configurations preceding fragmentations (i.e., MH-2 or MH-3) is a “regulator” in the overall reactions. One pathway is more sensitive than the other to structural changes in each series, and it depends on where (A- or B-ring) the substituents are attached. To gain further insight into the mechanism, we decided to make an authentic ion, MH-2, that resides in a different energy well on the potential energy surface, and also to examine the chemistry of deuterated chalcones, the MD<sup>+</sup> ions.

The 1,5-diketone compounds **16–19** (Chart 2) were then synthesized, and their MH<sup>+</sup> ions were subjected to collisional activation. The product ion of a major fragmentation, as shown in Scheme 3 for compound **17**, is exactly the MH-2 ion for the corresponding chalcone. As expected, the ion arising from this fragmentation of the 1,5-diketone molecules showed a CID mass spectrum *identical* to that of the corresponding protonated chalcone. Figure 5 exemplifies the spectrum for the *m/z* 223 ion from **17**, which is indistinguishable from that for **7** shown in Figure 1 (additional data can be found in the Supporting

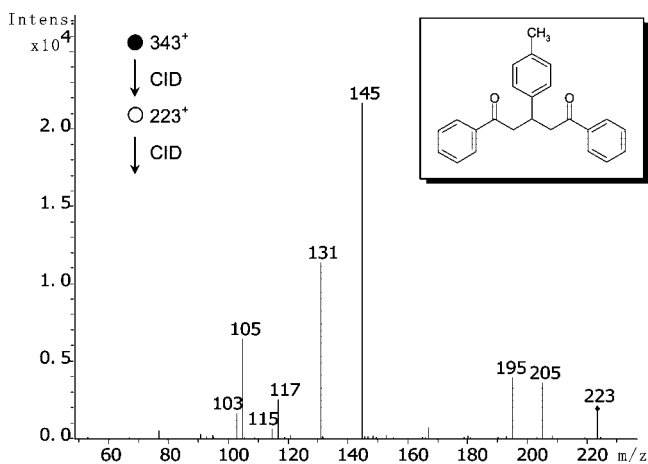


**FIGURE 5.** CID mass spectrum of the *m/z* 223 ion generated in fragmentation of the MH<sup>+</sup> ion (*m/z* 343) of **17**. This is identical to that shown in Figure 1 for **7**.

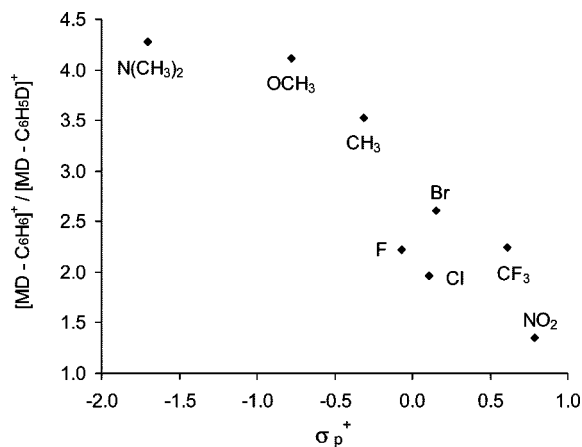


**FIGURE 6.** Losses of C<sub>6</sub>H<sub>6</sub> and C<sub>6</sub>H<sub>5</sub>D from the MD<sup>+</sup> ions of **2–9** in relation with the  $\sigma_p^+$  substituent constants.

Information). This is an indisputable evidence that, upon collisional activation, interconversion between MH-1 and MH-2 takes place prior to elimination of A-ring benzenes.

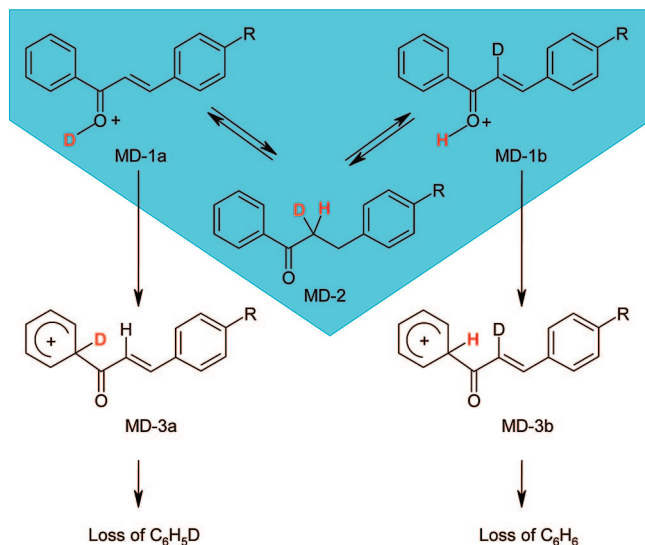
Another similar reaction, which is not the focus of this study, the loss of the B-ring benzenes (e.g., *m/z* 131 in Figure 1), involves proton transfer ultimately to the C<sub>1</sub>-position of the B-ring. Loss of benzene from this side indicates that the “extra” proton is floating among several positions, and once it hits a dissociative site, a fragmentation reaction follows.

Isotope labeling is always powerful in the studies of reaction mechanisms. In the CID mass spectra of the MD<sup>+</sup> ions of selected chalcones (series I), losses of C<sub>6</sub>H<sub>6</sub> and C<sub>6</sub>H<sub>5</sub>D (both of the A-ring) were observed, which was confirmed by the accurate mass determined on the ultrahigh resolution FT-ICR mass spectrometer (see Table S2 in the Supporting Information). This implies that the external deuterium and an internal hydrogen were competing in this reaction. More interestingly, it was found that the [MD - C<sub>6</sub>H<sub>6</sub>]<sup>+</sup>/[MD - C<sub>6</sub>H<sub>5</sub>D]<sup>+</sup> ratios varied with the substituent constants as illustrated in Figure 6 (note the linear scale). Early studies<sup>31</sup> on deuterated chalcones demonstrated that in loss of the A-ring benzene, H/D scrambling involving *ring* hydrogens was negligible. Given what we know now about the “regulator” role TS-12 plays (for series I), when the substituent is a strong electron-donating group (e.g., (CH<sub>3</sub>)<sub>2</sub>N or CH<sub>3</sub>O), a reduced energy barrier between MD-1 and MD-2 (refer to Figure 2) would allow their interconversion through TS-12 to mix the external deuterium and the *olefinic* hydrogen as shown in the shaded area in Scheme 4. However, the subsequent transfer of a deuterium on MD-1a or a proton on MD-1b via TS-13 for the reaction to proceed (Figure 2) will be marked by a considerable kinetic isotope effect, *k<sub>H</sub>/k<sub>D</sub>*. If interconversion between MD-1 and MD-2 were free (i.e., [MD-1a]/[MD-1b] = 1:1), then the [MD - C<sub>6</sub>H<sub>6</sub>]<sup>+</sup>/[MD - C<sub>6</sub>H<sub>5</sub>D]<sup>+</sup> intensity ratio would be the *k<sub>H</sub>/k<sub>D</sub>* value. From R = OCH<sub>3</sub> to R = N(CH<sub>3</sub>)<sub>2</sub>, this ratio increased only marginally despite the large change in the  $\sigma_p^+$  value. This plateau in intensity ratio changes probably implies that the interconversion is almost free for these two compounds, and the intensity ratios represent the majority of their *k<sub>H</sub>/k<sub>D</sub>* values.

As the electron-withdrawing power of the substituent increases, the energy barrier (TS-12) heightens and thus prevents

(31) (a) Ardanaz, C. E.; Traldi, P.; Vettori, U.; Kavaka, J.; Guidugli, F. *Rapid Commun. Mass Spectrom.* **1991**, *5*, 5–10. (b) Ardanaz, C. E.; Kavaka, J.; Curcuruto, O.; Traldi, P.; Guidugli, F. *Rapid Commun. Mass Spectrom.* **1991**, *5*, 569–573.

## SCHEME 4



complete interconversion, causing decrease in population of MD-1b and leaving MD-1a (the initial MD<sup>+</sup> ions) as the major component. Note that MD-1a leads *only* to MD-3a to lose C<sub>6</sub>H<sub>5</sub>D (Scheme 4), thus resulting in declining [MD – C<sub>6</sub>H<sub>6</sub>]<sup>+</sup>/[MD – C<sub>6</sub>H<sub>5</sub>D]<sup>+</sup> ratios shown in Figure 6. When R = NO<sub>2</sub>, this ratio is only 1.35. These results are likely to *rule out* the possibility that the MD-1 → MD-3 process takes place by an alternative 1,4-deuteron transfer to the *ortho* position of the A-ring followed by “hydrogen ring-walk”,<sup>21</sup> (since that would give the [MD – C<sub>6</sub>H<sub>6</sub>]<sup>+</sup>/[MD – C<sub>6</sub>H<sub>5</sub>D]<sup>+</sup> ratio ≥ 5 in *all* cases including R = NO<sub>2</sub> based on statistics). Therefore, this is additional evidence supporting the reaction mechanism presented in Figure 2 given by theoretical calculations.

**Dissociative Protonation.** In this study, we were more focused on the elimination of the A-ring upon protonation. It is interesting because this reaction requires that the C<sub>1</sub>-position on this ring be protonated to form the MH-3 ion (Scheme 1) even though the PA value at this site is significantly *lower* (by 25 kcal/mol, Figure 2) than that at the carbonyl oxygen. It is the dominant reaction for most of the chalcones studied (see Table S1 in the Supporting Information).

During theoretical calculations we found that upon protonation at the C<sub>1</sub>-position, the resulting MH-3 ion dissociates spontaneously. However, the two fragments are held together electrostatically as a stable cinnamoyl cation/benzene complex. As shown in Figure 7, in this complex, the neutral benzene is completely planar with six identical C–H bonds, and the distance between the two carbon atoms originally bonded is now 3.09 Å (versus 1.46 and 1.48 Å for the corresponding bond

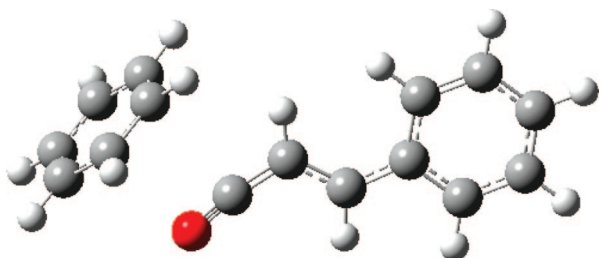


**FIGURE 7.** Optimized structure of the MH-3 ion formed upon protonation of the unsubstituted chalcone at the C<sub>1</sub>-position of the A-ring (the atom in red is oxygen).

in MH-1 and MH-2, respectively, Table S3 in the Supporting Information). This is a reaction intermediate that resides in a very shallow energy well (only 4 kcal/mol below the final products, Figure 2) as mentioned previously in other systems.<sup>20</sup> Although ion-neutral complexes<sup>32</sup> are common intermediates in fragmentation reactions in mass spectrometry, this cinnamoyl cation/benzene complex found here is formed upon protonation at a particular position that causes spontaneous dissociation, which is truly an excellent showcase in our search for dissociative protonation sites.

## Conclusions

In the mass spectrometry of chalcones, Ph-CO-CH=CH-Ph', loss of a benzene from either end and loss of styrene were observed as the major fragmentation reactions of the protonated molecules. It was found that the carbonyl oxygen was the most favorable site for protonation (which is, however, not dissociative) and proton transfer to a dissociative site was a regulator of the overall reactions. The substituent effect was used as a probe to examine the reaction mechanisms. It was also observed that the proton was floating among several positions, and fragmentation reactions took place once it hit dissociative sites. These dissociative sites included the C<sub>1</sub>-positions on both phenyl rings that triggered losses of the benzenes, even though they were thermodynamically unfavorable in protonation.

## Experimental Section

The chalcone compounds with a substituent either on the right B ring (series I) or the left A ring (series II), shown in Chart 1, were synthesized previously<sup>33</sup> following standard procedures for the Claisen-Schmidt reaction.<sup>34</sup> The 1,5-diketone compounds (Chart 2) were synthesized as described elsewhere.<sup>35</sup> The structures of all compounds were confirmed by <sup>1</sup>H and <sup>13</sup>C NMR and mass spectrometry.

Mass spectral data discussed here were obtained from an ion trap mass spectrometer operated in the positive ion mode with an atmospheric pressure chemical ionization (APCI) ion source and the software package provided by the vendor. The capillary voltage was set at –4000 V, and the ion source temperature was set at 400 °C. Nitrogen was used as the nebulizing gas, at a pressure of 15 psi, and as the drying gas at a flow rate of 5 L/min. CID mass spectra were obtained with helium as the collision gas at a collision energy achieved by a voltage of 0.7 V. Accurate mass was measured on an FT-ICR mass spectrometer (7.0 T) with an APCI ion source.

(32) General reviews on ion-neutral complexes: (a) Bowen, R. D. *Acc. Chem. Res.* **1991**, *24*, 364–371. (b) Longevialle, P. *Mass Spectrom. Rev.* **1992**, *11*, 157–192. (c) McAdoo, D. J.; Morton, T. H. *Acc. Chem. Res.* **1993**, *26*, 295–302.

(33) Tai, Y. P.; Pei, S. F.; Wan, J. P.; Cao, X. J.; Pan, Y. *J. Rapid Commun. Mass Spectrom.* **2006**, *20*, 994–1000.

(34) Smith, M. B. *Organic Synthesis*, 2nd ed.; McGraw-Hill: New York, 2002; p 740.

(35) Swamy, V. M.; Sarkar, A. *Tetrahedron Lett.* **1998**, *39*, 1261–1264.

(36) Frisch, M. J.; Trucks, G. W.; Schlegel, H. B.; Scuseria, G. E.; Robb, M. A.; Cheeseman, J. R.; Montgomery, J. A., Jr.; Vreven, T.; Kudin, K. N.; Burant, J. C.; Millam, J. M.; Iyengar, S. S.; Tomasi, J.; Barone, V.; Mennucci, B.; Cossi, M.; Scalmani, G.; Rega, N.; Petersson, G. A.; Nakatsuji, H.; Hada, M.; Ehara, M.; Toyota, K.; Fukuda, R.; Hasegawa, J.; Ishida, M.; Nakajima, T.; Honda, Y.; Kitao, O.; Nakai, H.; Klene, M.; Li, X.; Knox, J. E.; Hratchian, H. P.; Cross, J. B.; Adamo, C.; Jaramillo, J.; Gomperts, R.; Stratmann, R. E.; Yazyev, O.; Austin, A. J.; Cammi, R.; Pomelli, C.; Ochterski, J. W.; Ayala, P. Y.; Morokuma, K.; Voth, G. A.; Salvador, P.; Dannenberg, J. J.; Zakrzewski, V. G.; Dapprich, S.; Daniels, A. D.; Strain, M. C.; Farkas, O.; Malick, D. K.; Rabuck, A. D.; Raghavachari, K.; Foresman, J. B.; Ortiz, J. V.; Cui, Q.; Baboul, A. G.; Clifford, S.; Cioslowski, J.; Stefanov, B. B.; Liu, G.; Liashenko, A.; Piskorz, P.; Komaromi, I.; Martin, R. L.; Fox, D. J.; Keith, T.; Al-Laham, M. A.; Peng, C. Y.; Nanayakkara, A.; Challacombe, M.; Gill, P. M. W.; Johnson, B.; Chen, W.; Wong, M. W.; Gonzalez, C.; Pople, J. A. *Gaussian 03*; Gaussian, Inc.: Pittsburgh, PA, 2003.

The capillary voltage was set at  $-4300$  V, and the ion source temperature was set at  $350$  °C. Nitrogen was used as the nebulizing and drying gases, and argon was used as the collision gas.

All compounds were purified after synthesis and redissolved in acetonitrile or methanol containing 1% acetic acid at a concentration of approximately  $1$   $\mu\text{g/mL}$ . The solutions were infused into the ion source for analysis with a syringe pump at a flow rate of  $30$   $\mu\text{L/min}$ .

Theoretical calculations were performed by using the DFT method at the RB3LYP/6-31G(d) level of theory in the Gaussian 03 program.<sup>36</sup> The candidate structures of the reactants, products, and transition states were optimized by calculating the force constants. No symmetry constraints were imposed in the optimizations. The reaction pathways were traced forward and backward by the intrinsic reaction coordinates (IRC) method. All optimized structures were subjected to vibrational frequency analysis for zero-point energy (ZPE) correction to the temperature at  $298.15$  K and the pressure at  $1.0$  atm. The sum of electronic and thermal energies of the optimized structures were calculated.

**Acknowledgment.** We are gratefully indebted to a reviewer for his constructive and thoughtful comments that inspired us to revigorate the manuscript with additional data. This study was supported in part by the National Ministry of Education of China (NCET-06-0520) and NSFC of China (20776059).

**Supporting Information Available:** MS<sup>3</sup> spectra of the 1,5-diketo compounds **16–19** in comparison with the MS<sup>2</sup> spectra of the corresponding chalcones, mass spectral data for all chalcone compounds, accurate mass data for the product ions in the fragmentation of the MD<sup>+</sup> ions of compounds **5** and **8**, and DFT calculation results including geometries, total energies and Cartesian coordinates of the optimized structures. This material is available free of charge via the Internet at <http://pubs.acs.org>.

JO702464B